

Absorption enhancement in Amorphous Si by introducing RF sputtered Ti intermediate layers for photovoltaic applications

H. Ferhati[1], F. Djeffal[1,*], N. Boubiche[2], A. Benhaya[1], J. Faerber[3], F. Le Normand[2] and N. Javahiraly[2] and T. Fix[2]
[1] LEA, Department of Electronics, University of Batna 2, Batna 05000, Algeria
[2]MaCEPV/ ICube, Université de Strasbourg and CNRS, Strasbourg, France
[3] IPCMS, Université de Strasbourg and CNRS, Strasbourg, France
E-mails: faycal.djeffal@univ-batna2.dz
Tel/Fax: 0021333805494

Abstract

In this paper, embedded Amorphous-Silicon (*a-Si*) and Titanium (*Ti*) ultrathin-films forming a multilayer structure is proposed as a new efficient absorber material for thin-film solar cells (*TFSCs*). Promising design strategy based on combining *FDTD* (*Finite Difference Time Domain*) with Particle Swarm Optimization (*PSO*) was adopted to identify the *a-Si/Ti* multilayer geometry offering the highest Total Absorbance Efficiency (*TAE*). It is found that the optimized design can serve as an effective absorber, yielding superb *TAE* exceeding *80%*. The optimized *a-Si/Ti* multilayer was then elaborated by successive growth of *a-Si* and *Ti* ultrathin layers using *RF* magnetron sputtering technique. The sputtered *a-Si/Ti* thin-film was characterized by Scanning Electron Microscopy (*SEM*), *X*-ray diffraction (*XRD*), and *UV-Visible* absorption spectroscopy. Measurements showed a unique optical behavior, promoting broadband absorbance over the visible and even *NIR* spectrum ranges. In particular, the prepared *a-Si/Ti* absorber exhibits an optical band-gap of *1.36 eV*, which is suitable for photovoltaic applications. A performance assessment of the elaborated absorber was investigated by extracting *I-V* characteristics and electrical parameters under dark and *1-sun* illumination. It is revealed that the proposed absorber demonstrates outstanding electrical and sensing performances. Therefore, promoting enhanced resistive behavior and light-scattering effects, this innovative concept of optimized *a-Si/Ti* multilayer provides a sound pathway for designing promising alternative absorbers for the future development of *a-Si*-based *TFSCs*.

Key words: broadband; *RF* sputtering; Titanium; *a-Si*; absorber; photovoltaic.

1. Introduction

Nowadays, the worldwide energy production moves towards exploring clean energy resources to eventually replace exhaustible and polluted fossil fuels ones, which could open up new pathways to develop sustainable economic growth. Particularly, Photovoltaic (*PV*) technology has been a topic of interest in the last half century because of its ability for providing viable carbon-neutral energy [1-3]. However, the actual stage of maturity of *PV* systems calls for a renewed performance assessment to make them competitive with fossil fuels concerning utility-scale energy generation [2-4]. Till now, crystalline Silicon (*c-Si*) *PV* technology dominates the commercialization market as compared to its counterpart based on thin-film material (*CdTe*, *CIGS*, *CZTS* and *a-Si*) [4-8]. Having benefited from decades of intensive research efforts, *c-Si*-based technology demonstrates an improved efficiency that exceeds *26%* and high-level of maturity at the industrial view point [9]. However, the use of very thick (*180–300 μm*) *Si*-absorbers and expensive thermal processing can increase the production cost, which constitutes its major problem for replacing carbon-energy resources. For this purpose, a major research and development focus has been devoted to design thin-film solar cells with absorber thicknesses in the range *1–2 μm* in order to reduce the elaboration cost of the *PV* module, while maintaining a high conversion efficiency approaching the Shockley-Queisser limit [5-8]. In this perspective, various strategies based on nanostructures, heterojunction, multilayers, tandem configuration, electrode engineering and band-gap grading have been proposed to improve the efficiency of thin-film solar cells [10-16]. Although the fact that these aspects have enabled exciting opportunities for reaching higher efficiencies, the scarcity of some elements, the processing complexity and the use of toxic materials constitute the main bottlenecks for their eventual deployment for building efficient *PV* panels.

Silicon thin-film solar cells have shown widespread production in comparison to other inorganic thin films [9], [15-16]. Accordingly, *a-Si:H*-based technology is attractive, being able to provide a favorable efficiency value of *10.2%* with low production cost [17]. Even though these fascinating properties, *a-Si:H*-based solar cells face strong pressure to compete it counterparts based on *c-Si* materials in terms of efficiency/cost ratio, and even stability [18-20]. This passes inevitably through avoiding various problems associated with this technology. Among these challenges, the *a-Si:H* material is considered more defective than *c-Si* because of the high density of defects, thus significantly deteriorating the solar cell performance. In addition, this technology suffers from the degradation-related to Staebler-Wronski effects (*SWEs*), affecting the solar cell stability [21-24]. Besides, the elaboration of this kind of thin-film inorganic solar cells necessitates the use of SiH_4 toxic material. On the other hand, the *a-Si:H* technology exhibits extensive optical losses over a wide spectrum range, which is attributed to its relatively high band-gap (*1.7eV-1.9eV*) [19]. Therefore, engineering the *a-Si* cells so that sunlight is trapped inside to reach a broadband absorbance behavior is extremely important. Also, designing high-performance innovative absorbers based on free critical raw material (*CRM*) technology, that involves nontoxic, earth-abundant and eco-friendly constituents, becomes more realistic [25]. Motivated by this concept, the present work aims at developing a new environment-friendly and low-cost absorber material for thin-film solar cell applications. Accordingly, *a-Si/Ti* multilayer structure acting as efficient absorber was prepared using *RF* magnetron sputtering technique. The latter approach allows avoiding the use of toxic SiH_4 material to prepare *a-Si*-based absorbers. Before the elaboration of the proposed *a-Si/Ti* absorber, a strategic combination of *PSO* and numerical analysis is used to find out the best geometry offering superior *TAE*. Morphological, structural, optical and electrical characterizations of the optimized *a-Si/Ti* thin-film were carried out. It is found that the prepared *a-Si/Ti* multilayer shows outstanding absorption capabilities over a wide spectrum range with enhanced electrical performances. Therefore, this innovative concept provides a sound pathway for designing promising alternative absorbers of new *a-Si*-based *TFSCs.*

2. Design, optimization and experiments

In this section, we have versatile objectives mainly represented by two-stage investigation frameworks of a new absorber based on *a-Si/Ti* multilayer structure for photovoltaic applications. The first objective relies on a strategic combination of accurate numerical modeling and *PSO* global optimization to design a high-performance *a-Si*-based absorber, while the second one is devoted to the fabrication and characterization of the optimized *a-Si/Ti* multilayer design using the *RF* magnetron sputtering technique.

2.1 Device design and optimization

The cornerstone of the investigated absorber based on non-hydrogenated *a-Si* dwells on introducing intermediate *Ti* metallic sub-layers, forming a multilayer structure. In this framework, Fig.1 (a) depicts a cross-sectional view of the proposed *a-Si/Ti* multilayer absorber layer, where highly transparent *ITO* layer for which its thickness is denoted by t_{ITO} is introduced at the top of the structure to enhance the reduce reflection losses. Embedded *a-Si* and *Ti* thin-films are considered on a glass substrate, where $t_{a-Si} = [t_{Si1}, t_{Si2}, ..., t_{Sin}]$ *and* $t_{Ti} = [t_{Ti1}, t_{Ti2}, ..., t_{Tij}]$ are the victors of the thickness values associated with the successive silicon and titanium layers. The thickness of the entire absorber thin-film is $t_{Absorber}$.

As far as we are concerned, designing high-performance thin-film solar cells through intuiting the absorber material structural, electrical and geometrical parameters based on well understanding of the physical rules and limitations that govern the behavior of the specified photovoltaic technology is not sufficient to achieve the best performances. Alternatively, we believe that sophisticated numerical optimization strategies behaving like predictive simulations are required to forecast the thin-film solar cell performance. Accordingly, global optimization using compact numerical modeling of the *TFSCs* absorber could principally transform the design step towards a search problem, where taking into account the performance *FoMs* and the effects causing the optical losses yields an effective pathway to design perfect absorbers with minimal guesswork. In this perspective, the *PSO*-based metaheuristic technique can be applied to optimize the optical performance of the proposed *a-Si/Ti* multilayer absorber [25]. This technique is extensively employed to perform effective predictive simulations, which allow optimizing and outperforming various nanoelectronic and optoelectronic devices [26-28]. The main objective of our investigation consists of a strategic combination between *PSO* approach and an accurate numerical analysis to identify the best geometry associated with the investigated *Si/Ti* multilayer structure that could enable achieving the highest *TAE*, while maintaining enhanced antireflection capabilities. In this context, the flowchart shown in Fig.1 (b) illustrates the adopted hybrid methodology based on combined *PSO* and numerical modeling approaches. The absorber optical behavior is modeled using *SILVACO* software [29], in which the associated absorbance, reflectance and *TAE* parameters are carried out using *2D-FDTD* method. More details regarding the suggested modeling approach and the *PSO* metaheuristic technique can be found in our previously published works [26] and [32], where the *TAE* formula is given by:

$$TAE = \frac{\int_{\lambda_{\min}}^{\lambda_{\max}} \frac{\lambda}{hc} A\left(\lambda\right) P_i\left(\lambda\right) d\lambda}{\int_{\lambda_{\min}}^{\lambda_{\max}} \frac{\lambda}{hc} P_i\left(\lambda\right) d\lambda} \qquad (1)$$

where *A* is the absorbance, *h* refers to the Plank's constant, *c* is the light velocity, λ represents the wavelength and $P_i(\lambda)$ is the solar spectral irradiance, which can be approximated by a well known non-linear function presented in [30].

An objective function for the *PSO* global optimization is formulated by considering two goals with respect to the solar cell optical behavior. In other words, the investigated *a-Si/Ti* multilayer structure is optimized by satisfying the maximization of the absorbance over a wide spectrum range, while reducing the structure reflection losses. Therefore, by considering a mono-objective global optimization scheme based on weighting coefficients, the fitness function is given by:

$$Fitness\ (X) = w_1 \frac{1}{TAE} + w_2 R \qquad (2)$$

where R is the reflectance coefficient, $X_i = (t_{a-Si} = [t_{Si1}, t_{Si2}, ..., t_{Sin}], t_{ITO}, t_{Ti} = [t_{Ti1}, t_{Ti2}, ..., t_{Tij}], j)$ of the i^{th} generation represents the design parameter vector, n is the number of the multilayer layers with j denotes the number of the *Ti* intermediate metallic thin-films and w_i *(i = 1-2)* are weighting coefficients considered to be equal to *1/2*.

The stall generation and the population size of the *PSO* technique are respectively taken with *20* and *1500*. The evolution of the normalized fitness function as a function of the number of generation associated with the *PSO* metaheuristic technique is shown in Fig.1 (c). It can be seen that a good stabilization is reached for *850* generation and the *TAE* is appropriately maximized, proving the effectiveness of global optimization approach for designing perfect *a-Si*-based absorbers. As a result, the optimized design is given by $X_i = (t_{a-Si} = [18nm, 10nm, 10nm, 22nm, 51nm], t_{ITO} = 25nm, t_{Ti} = [17nm, 22nm, 23nm, 21nm, 28nm], j = 5)$. It is found that the latter geometry of the analyzed *a-Si/Ti* multilayer structure can provide a high *TAE* exceeding *81.5%* over the wavelength range of [*300 nm-1100 nm*]. This emphasizes the effectiveness of the proposed approach for promoting efficient light management, thus enabling the opportunity to design high-performance *a-Si*-based absorbers for *TFSCs* application. We believe that experiments supported by efficient numerical optimization can open up exciting opportunities for realizing efficient absorbers. Therefore, the next step is dedicated to the elaboration of the optimized *a-Si/Ti* multilayer structure, which constitutes the main goal of the next sub-section.

2.2 Experimental details

The optimized *a-Si/Ti* multilayer structure was fabricated by three-step manufacturing processes. In the beginning, Glass substrates were ultrasonically cleaned up by using *10 min* sequential sonication process in acetone and ethanol, then rinsed in heated de-ionized water at *90°C* and dried under a nitrogen jet procedure. Thereafter, successive deposition of *a-Si* and *Ti* thin-layers with the optimized geometry on the glass substrate was carried out by means of *RF* magnetron sputtering technique using *MOORFIELD MiniLab 060*, in which *p*-type *Si* and *Ti* targets with high purity of *99.99%* were used. This technique is considered efficient for depositing several thin-film materials [17], [19] and [31-32]. The sputtering process of the *a-Si/Ti* multilayer stack was performed in an atmosphere containing *Ar* gas with a pressure of *1.5 Pa*. Besides, the substrate to targets distance was kept at *6.5 cm* for the Titanium, while it was fixed at *5.1 cm* for the *Si* material. The source power was maintained at *520 W* during the sputter-deposition process of the optimized *a-Si* and intermediate *Ti* sub-layers. The deposition rate of the *a-Si* and *Ti* layers were respectively *0.13 nm/s and 0.10 nm/s.* The thickness of the *Ti* and of the *a-Si* thin-films was designed as it is outlined in the last sub-section. Each layer is separately grown on a glass substrate first to calibrate and to optimize the *RF* sputter-deposition process in order to reach the accurate geometry of the optimized multilayer stack design. The substrate temperature was kept at *300K* during the sputtering process. Then, an *ITO* ultrathin film was grown on the sputtered *a-Si/Ti* multilayer via *RF* sputtering and by using targets with *90 wt%* In_2O_3 and *10 wt%* SnO_2. The sputtering process was carried out in a mixture atmosphere of *Ar* and O_2 (*Ar: 66%,* O_2*: 33%*). The *RF* source power was kept at *250 W* and the working pressure was set to *1.33 Pa*, resulting in a deposition rate of *0.20 nm/s*. The distance between *ITO* targets and *a-Si/Ti/Glass* sample was

6.8 cm. The thickness of the sputtered *ITO*, *a-Si* and *Ti* sub-layers were calculated by ellipsometric measurement. For comparison purposes, it is worth mentioning that *ITO*/*a-Si* thin-film sample was also fabricated to show the role of the proposed design amendment on the optical and electrical properties of the *a-Si*-based absorber.

The morphological characteristics of the prepared *a-Si/Ti* multilayer stacked structure were analyzed using Scanning Electron Microscopy (*SEM*), where the surface (top) and the cross-section (side) prepared by ion bombardment were imaged with a Zeiss Gemini *SEM* 500 with a Field Emission Schottky source equipped with an *EDAX SDD* for chemical analysis. The structural properties of the prepared multilayer thin-films were also characterized by *X*-ray diffraction (*XRD*) measurements (*ARL Equinox 3000*) for 2θ diffraction angle scans of [*25°- 80°*]. The spectrophotometer (*F10-RT-UV*) was used to extract the *UV-Vis-NIR* absorbance and reflection spectra of the fabricated absorber based on *a-Si/Ti* multilayer structure. Moreover, the absorber degradation behavior related to illumination effect at different periods was investigated by measuring the evaluation of the structure *TAE* as a function of the time of *1-sun* light exposure. The semiconductor characterization system (*Keithley 4200-SCS*) was exploited to measure the *I-V* characteristics under dark and *1-sun* illumination conditions and the absorber electrical parameters were extracted.

3. Results and discussions

3.1 Morphological and structural characteristics

The morphological analysis of the elaborated absorber based on *a-Si/Ti* multilayer structure seems important and can provide a global insight concerning its optical behavior. In this framework, Fig.2 shows the *SEM* top surface (a) and cross-sectional (b) images of the prepared sample with embedded *a-Si* and *Ti* sputter-deposited thin-films. It can be observed from the obtained *SEM* images that the absorber structure, including the *a-Si/Ti* nano-multilayers and the *ITO* film from the glass substrate to the surface, could be obviously discerned, where a series of layers showing by contrast the *a-Si*, the titanium and the *ITO* can be identified as it is described in Fig.2 (b). The careful analysis of the cross-sectional image demonstrates that we were able to identify *8* observable and continuous films of the *12* sputter-deposited layers constituting the *a-Si/Ti* multilayer as it is illustrated in Fig.1 (a), while the stacked *a-Si* and *Ti* layers near the surface $[t_{Si2}, t_{Si3}, t_{Ti1}, t_{Ti2}]$ are not continuous. This indicates that the growth is essentially columnar for these ultrathin films, which led to roughness development for the last deposited very thin layers. The profilometer measurements outlined that the thicknesses of the identified *a-Si* layers were *20 nm, 21 nm, 24 nm* and *49 nm* respectively from the substrate to the top surface of the prepared absorber, while the thicknesses of the observable *Ti* intermediate layers were respectively *20 nm, 22 nm* and *26 nm*. In addition, Fig.2 (a) shows accordingly that the deposited *ITO* film exhibits inter column porosity with surface roughness characteristics. The explanation can be as follows: as the sub-layers forming the multilayer structure are stacked by sputtering method, the roughness increases considerably and when the grain size is larger than the layers thickness, the growth becomes columnar with non-perfect continuity as it is shown for the sputtered layers closest to the surface.

The crystalline structure of the elaborated absorber designs with *ITO/a-Si* and *a-Si/Ti* multilayer structures was examined using *X*-ray diffraction measurements. Accordingly, Fig.3 illustrates *XRD* patterns for (2θ) diffraction angle ranging from *25°* to *80°* of the prepared samples: (a) the conventional *ITO/a-Si* structure and (b) the prepared absorber based on embedded *a-Si* and *Ti* ultrathin films. It can be seen from this figure that low-intensity *XRD* peak at the diffraction angle around *31°*, matching the (*222*) facet of *ITO* material is observed. Fig.3 (a) indicates also the presence of silicon microcrystals following the (*111*) orientation, with a low intensity peak at the diffraction angle of *28.5°*. In fact, the sputtering of relatively thick *Si* layers allows the formation of *Si* crystallized microstructures. On the other hand,

Fig.3 (b) demonstrates the amorphous state of the silicon and *ITO* sputtered layers associated with the prepared absorber with multilayer structure, where no coherent *XRD* peaks are matching these materials. This observation correlates with previous published works that investigated the structural characteristics of sputtered *a-Si* [18-20]. The obtained structural properties can be explained by a mixture of two effects, firstly, the ultralow thickness of the deposited silicon sub-layers preventing the crystallization of the *Si* material. Secondly, the increased roughness induced by the growth of multilayered structure as it is confirmed in Fig.2. Besides, low-intensity *XRD* peak associated with *Ti* material from the (*101*) plan is observed around *39.5°*, emphasizing the beginning of the crystallization phase of the deposited *Ti* sub-layers.

3.2 Optical properties

UV-Vis-NIR spectroscopy analysis was used to investigate the influence of the *a-Si/Ti* multilayer structure with optimized geometry on the optical behavior of the prepared thin-film based absorber. In this context, Fig.4 (a) illustrates the absorbance spectra associated with the elaborated samples based on conventional *ITO/a-Si* structure and the stacked *a-Si* and *Ti* ultrathin layers. It is clearly shown from these spectra that the prepared absorber based on multilayers with optimized *Ti* intermediate metallic thin-films demonstrates broad-band absorption over the visible spectrum range. Besides, the absorbance decreases slightly over *NIR* spectrum range to reach *70%*. Interestingly, the prepared *a-Si/Ti* multilayer structure outperforms greatly the conventional design in terms of the absorbance capability, where it yields a high *TAE* exceeding *85%*. This is basically due to the enhanced light-trapping capability promoted by the use of optimized multilayer structure, where the adopted hybrid approach based on the strategic combination of embedded *a-Si* and *Ti* sub-layers and *PSO* global optimization procedure enables achieving an improved light-management. Moreover, the introduction of *Ti* inter-layers with optimized geometry induces optical nano-cavities leading to confine more light within the *a-Si* sub-layers thereby enhancing the *Vis-NIR* absorbance efficiency. More importantly, further improvements concerning the absorber optical behavior are recorded due to the resulted columnar morphology of the multilayer near the structure surface as it is above-discussed, which could plays a crucial role in promoting enhanced light-scattering effects. This leads to extend the optical path, thus providing wider possibilities for the incident photons to be absorbed.

To get a profound insight concerning the light absorbing property of the elaborated *a-Si/Ti* multilayer-based absorber, the absorption coefficient α has been calculated and illustrated in Fig.4 (b). It can be seen from the latter figure that the proposed absorber with stacked *a-Si* and *Ti* metal layers exhibits an enhanced absorption coefficient as compared to the conventional structure. The absorption coefficient increases with energy increase when the edge of absorber band gap is achieved. The obtained absorption coefficient of the elaborated absorber exceeds $10^5\ cm^{-1}$, which is comparable to that of the *c-Si* commercially dominating absorber, and superior than other promising materials for photovoltaic applications. This enhancement is attributed to the above-mentioned effects of improved light-trapping capability that promotes enhanced absorbance efficiency. The optical band gap of the elaborated absorbers based on *ITO/a-Si* and *a-Si/Ti* multilayer structures was calculated using the Tauc plots displayed in Fig.4 (c). The photon energy interval corresponding to the strong absorption capability of both prepared absorbers [*1.2 eV -2.8 eV*] is selected for the analysis. It was revealed that the elaborated absorber with stacked *a-Si* and *Ti* layers exhibits an appropriate band gap of *1.37 eV*. The latter value is close to the optimal value of *1.5 eV* highly suitable for solar absorber application. On the other hand, the conventional *a-Si* film shows an optical band gap of *2.07 eV*, which is found in good agreement with recently published works concerning sputtered *a-Si* thin-films [19]. It is to note that a good reliability for the performed analysis is reached, where the correlation factor for straight-line fit is about *0.98* for both samples. Therefore, the appropriate optical band gap and the high absorption coefficient make the elaborated *a-Si/Ti* sputter-deposited multilayer structure quite promising absorber for *TFSCs* application.

It is believed that the performance assessment of *a-Si*-based absorbers for photovoltaic application passes inevitably through evaluating its reliability and stability against the degradation induced by illumination effects [21-24]. In this context, Fig.5 (a) depicts the measured absorbance spectra associated with the elaborated absorber with optimized multilayer as a function of ageing under *1*-sun illumination in dry air. This figure outlines that by increasing the illumination time, the absorbance degrades at a significantly slower rate. Fig.5 (b) displays the variation of the total absorbance efficiency as a function of the irradiation time. It is apparent from this figure that the degradation of *TAE* is rather linear with slow descendant tendency. This figure demonstrates also that the elaborated absorber offers a high reliability and stability against light-induced degradation effects, where the *TAE* degrades with only *2.2%* after *20* hours under *1*-sun light exposure. In fact, when the absorber material is illuminated under long duration, weak bonds will be broken, inducing defects that can in turn degrade the absorber performances [22]. This effect is not highly pronounced for the elaborated sample due to the absence on weak hydrogen-silicon bonds. Moreover, the use of low thickness layers with multilayer structure can relatively reduces the defect density in the absorber, thus enabling reduced degradation related to light illumination effects. Therefore, the proposed *a-Si/Ti* multilayer structure shows a good stability further confirming its outstanding performances as a solar cell absorber.

3.3 Electrical characteristics

The recorded fascinating structural and optical properties of the prepared *a-Si/Ti* multilayer structure as it is thoroughly discussed in previous sub-sections have inspired the investigation of its photoelectrical sensing performances. For this purpose, the previously investigated samples were prepared as device structure based on the Metal/Semiconductor/Metal Schottky diode configuration. Accordingly, the schematic representation of the fabricated *Au/a-Si-Ti multilayer/Au* device structure is depicted in Fig.6 (a), which was used to study the absorber photoresponse under *1*-sun illumination. Top and bottom gold contacts were achieved via e-beam evaporation technique. The current-voltage characteristics under dark and illumination conditions of both prepared samples were measured and depicted in Fig.6 (b) and (c) respectively. In this context, Fig.6 (b) shows that the prepared device based on *a-Si/Ti* multilayer aspect exhibits higher dark current as compared to the conventional structure based on *a-Si* thin-film. This behavior is correlated to the presence of *Ti* metallic layers that contribute in enhancing the resistive behavior of the structure. On the other hand, it can be observed from Fig.6 (c) that the prepared device based on embedded *a-Si* and *Ti* sub-layers provides higher photocurrent under *1*-sun irradiation as compared to the conventional structure by 2-3 orders of magnitude, thus emphasizing the improved photoresponse of the proposed absorber. This enhancement can be explained by the improved absorbance efficiency as it is outlined in the section *3.2*. Furthermore, the use of multilayered design with metallic intermediate layers paves the way to extend the depletion region leading to enhancing the collection efficiency. In order to assess this hypothesis, we investigated in a more systematic way the electrical performances of the prepared absorbers based on stacked *a-Si* and *Ti* layers and conventional *a-Si* thin-film, where the electrical parameters including the series resistance, the Schottky barrier height and the ideality factor were extracted from the measured *I-V* curves using the characterization methodology reported in [32]. The obtained electrical parameters are subsequently summarized in Table.1. It is demonstrated from this table that the elaborated absorber with *a-Si/Ti* multilayer provides higher Schottky barrier height, further explaining the improved collection efficiency of the proposed structure as compared to the conventional *a-Si*-based absorber. In addition, it is revealed that the insertion of *Ti* intermediate layers enables enhancing the absorber conductivity, where it yields a low series resistance of *8.6 k*Ω as compared to that of thin-film *a-Si*. This outstanding result indicates that the proposed multilayer structure can be used as an effective strategy to enhance the solar cell fill factor which is considered as a big issue in *a-Si*-based *TFSCs* [19]. Therefore, we truly believe that the presented comprehensive investigation could give new perspectives for the realization of new low-cost and efficient absorber structures, which could be highly attractive for next-generation *a-Si*-based *TFSCs* application.

4. Conclusion

In summary, a new absorber material based on stacked *a-Si* and *Ti* ultrathin-films is proposed. The optical properties of the investigated *a-Si/Ti* structure geometry were firstly optimized using a strategic combination between *PSO* technique and *FDTD* method. The optimized multilayer absorber material was then prepared by sputtering and *SEM*, *XRD* and *Vis-NIR* spectroscopy measurements were carried out and thoroughly discussed to assess the morphological, structural and optical characteristics of the elaborated multilayer structure. It was found that near perfect *Vis-NIR* absorbance with over than *85%* of *TAE* and absorption coefficient exceeding $10^5\ cm^{-1}$ could be easily tuned by considering embedded *a-Si* and *Ti* ultrathin-films. This is mainly attributed to the effective light-management promoted by the optimized multilayer structure. The absorber reliability against light-induced degradation effects was investigated, where it was found that the prepared *a-Si*-based absorber shows an ultralow degradation of only *2.2%* for *20* hours under *1-sun* light exposure. Moreover, the absorber photoelectrical properties were analyzed. It was revealed that the prepared multilayered absorber demonstrates a high photoresponse as compared to the conventional *a-Si* thin-film, which is correlated to the reduced series resistance and optical losses. Therefore, these interesting properties of such engineered *a-Si/Ti* multilayer structure enable it to be a potential alternative absorber for future *TFSCs* and solar energy applications.

Acknowledgement

The authors gratefully acknowledge the financial support of General Directorate for Scientific Research and Technological Development (DGRSDT), Algeria.

References

[1] D. Batibay, Y. S. Ocak, M. F. Genisel and R. Turan, "Co-sputtered Cu2ZnTi(S:Se)4 absorbers for thin film solar cells," Renewable Energy, vol.145, pp. 1672-1676, 2020.

[2] K. Branker, M. Pathak and J. M. Pearce, "A review of solar photovoltaic levelized cost of electricity," Renew. Sustain. Energy Rev., vol. 15, pp.4470-4482, 2011.

[3] C. E. Pachón, L.F. Mulcué-Nieto, E. Restrepo, "Effect of band alignment on the n-InAlN/p-Si heterojunction for solar cells: a numerical study," Materialstoday Energy, vol.17, pp. 100457, 2020.

[4] P. K. Nayak, S. Mahesh, H. J. Snaith and D. Cahen , "Photovoltaic solar cell technologies: analysing the state of the art," Nature Review Materials, vol. 4, pp. 269-285, 2019.

[5] M. A. Green, "Tracking solar cell conversion efficiency," Nature Reviews Physics, vol. 2, pp. 172–173, 2020.

[6] K. Kacha, F. Djeffal, H. Ferhati, D. Arar, M. Meguellati, " Numerical investigation of a double-junction a: SiGe thin-film solar cell including the multi-trench region," Journal of Semiconductors, vol. 36,pp. 064004, 2015.

[7] J. Ramanujam, D. M. Bishop, T. K. Todorov, O. Gunawan, J. Rath, R. Nekovei, E. Artegiani and A. Romeo, "Flexible CIGS, CdTe and a-Si:H based thin film solar cells: A review," Progress in Materials Science, vol.110, pp. 100619, 2020.

[8] W. Wang, M. T. Winkler, O. Gunawan, T. Gokmen, T. K. Todorov, Y. Zhu, D. B. Mitzi, Device "Beyond 11% Efficient Sulfide Kesterite $Cu_2Zn_xCd_{1-x}SnS_4$ Solar Cell: Effects of Cadmium Alloying," ACS Energy Lett., vol.2, pp.930-936, 2017.

[9] M. A. Green, E. D. Dunlop, J. Hohl-Ebinger, M. Yoshita, N. Kopidakis A. W. Y. Ho-Baillie , "Solar cell efficiency tables (Version 55)," Progress In Photovoltaics, vol.28, pp. 3-15, 2020.

[10] H. Ferhati, F. Djeffal and K. Kacha, "Optimizing the optical performance of ZnO/Si-based solar cell using metallic nanoparticles and interface texturization," Optik, vol. 153, pp. 43-49, 2018.

[11] D. Yang, X. Zhao, Y. Liu, J. Li, H. Liu, X. Hu, Z. Li, J. Zhang, J. Guo, Y. Chen and B. Yang, "Enhanced thermal stability of solar selective absorber based on nano-multilayered AlCrSiO films, Sol. Energy Mater. Sol. Cells, vol.207, pp. 110331, 2020.

[12] H. Ferhati and F. Djeffal, "Graded band-gap engineering for increased efficiency in CZTS solar cells," Optical materials, vol.76, pp. 393-399, 2018.

[13] M. C. Beard, J. M. Luther and A. J. Nozik, “The promise and challenge of nanostructured solar cells,” Nature Nanotechnology, vol. 9, pp. 951–954, 2014.

[14] H. Ferhati, F. Djeffal, N. Boubiche and F. Le Normand, “An efficient ITO-free transparent electrode based on diamond-like carbon with an engineered intermediate metallic thin-film”, Solar Energy, vol. 196, pp. 327-335, 2020.

[15] N. Ahmed, P. Ramasamy, P. B. Bhargav, A. Rayerfrancis, B. Chandra, “Development of silicon nanowires with optimized characteristics and fabrication of radial junction solar cells with <100nm amorphous silicon absorber layer,” Materials Science in Semiconductor Processing, vol. 106, pp. 104778, 2020.

[16] W. Li, Y. Cai, L. Wang, P. Pan, J. Li, G. Bai and Q. Ren, “Fabrication and characteristics of N-I-P structure amorphous silicon solar cells with CdS quantum dots on nanopillar array,” Physica E: Low-dimensional Systems and Nanostructures, vol. 109, pp. 152-155, 2019.

[17] H. Sai, T. Matsui, H. Kumagai and K. Matsubara, “Thin-film microcrystalline silicon solar cells: 11.9% efficiency and beyond”, Applied Physics Express, vol. 11, pp. 022301, 2018.

[18] E. Márquez, E. Saugar, J. M. Díaz, C. García-Vázquez, S. M. Fernández-Ruano, E. Blanco, J. J. Ruiz-Pérez and D. A. Minkov, “The influence of Ar pressure on the structure and optical properties of nonhydrogenated a-Si thin films grown by rf magnetron sputtering onto room temperature glass substrates”, Journal of Non-Crystalline Solids, vol. 517, pp. 32-43, 2019.

[19] M. Stuckelberger, R. Biron, N. Wyrsch, F-J. Haug and C. Ballif, “Review: Progress in solar cells from hydrogenated amorphous silicon,” Renewable and Sustainable Energy Reviews, vol. 76, pp. 1497–1523, 2017.

[20] K. Liu, W. Yao, D. Wang, D. Ba, H. Liu, X. Gu, D. Meng, G. Du, Y. Xie and Y. Ba, “A study of intrinsic amorphous silicon thin film deposited on flexible polymer substrates by magnetron sputtering,” Journal of Non-Crystalline Solids, vol. 449, pp. 125-132, 2016.

[21] M. H. Elshorbagy, E. López-Fraguas, J. M. Sánchez-Pena, B. García-Cámara, R. Vergaz, “Boosting ultrathin a-Si-H solar cells absorption through a nanoparticle cross-packed metasurface,” Solar Energy, vol. 202, pp. 10-16, 2020.

[22] I. Pola, D. Chianese, L. Fanni and R. Rudel, “Analysis of annealing and degradation effects on a-Si PV modules, ” In Proc. of the 23rd European Photovoltaic Solar Energy Conference, December, 2008.

[23] N. Aristidou, C. Eames, I. Sanchez-Molina, X. Bu, J. Kosco, M. S. Islam and S. A. Haque, “Fast oxygen diffusion and iodide defects mediate oxygen-induced degradation of perovskite solar cells,” Nature Communications, vol. 8, pp. 15218, 2017.

[24] P. Arce et al, “Direct and inverse Staebler–Wronski effects observed in carbon-doped hydrogenated amorphous silicon photo-detectors,” Nuclear Instruments and Methods in Physics Research Section A: Accelerators, Spectrometers, Detectors and Associated Equipment, vol. 632, pp. 164-166, 2011.

[25] M. Clerc, J. Kennedy, “The particle swarm - explosion, stability, and convergence in a multidimensional complex space,” J. IEEE Trans. Evolut. Comput., vol. 73, pp. 6-58, 2002.

[26] H. Ferhati and F. Djeffal, “Exceeding 30% efficiency for an environment-friendly tandem solar cell based on earth-abundant Se/CZTS materials,” Physica E: Low-dimensional Systems and Nanostructures, vol.109, pp. 52-58, 2019.

[27] F. Djeffal and H. Ferhati, “A new high-performance phototransistor design based on both surface texturization and graded gate doping engineering,” Journal of Computational electronics,vol. 15, pp. 301-310, 2016.

[28] F. Djeffal, H. Ferhati “Planar junctionless phototransistor: A potential high-performance and low-cost device for optical-communications,” Optics and Laser Technology, vol. 97, pp.29-35, 2017.

[29] Atlas User’s manual, SILVACO TCAD, 2012.

[30] A. Benmir, M. S. Aida, “Analytical modeling and simulation of CIGS solar cells, Energy Procedia,” vol. 36, pp. 618-627, 2013.

[31] S. Y. Lee, Y. S. Park, T. Seong, “Optimized ITO/Ag/ITO multilayers as a current spreading layer to enhance the light output of ultraviolet light-emitting diodes,” J. Alloy. Compd., vol.776, pp. 960-964, 2019.

[32] A. Benhaya, F. Djeffal, K. Kacha, H. Ferhati, A. Bendjerad, “Role of ITO ultra-thin layer in improving electrical performance and thermal reliability of Au/ITO/Si/Au structure: An experimental investigation,” Superlattices and Microstructures, vol.120, pp. 419-426, 2018.

Figures caption:

Figure.1: (a) Cross-sectional view of the investigated absorber based on *a-Si/Ti* multilayer structure. **(b)** Flowchart of the adopted hybrid approach used to optimize the geometry of the proposed *a-Si/Ti* multilayer structure. **(c)** Evolution of the fitness function against generations of the *PSO*.

Figure.2: *SEM* images of **(a)** top (surface) and **(b)** cross-section of the elaborated *a-Si/Ti* multilayer structure using *RF* magnetron sputtering technique. The same scale bar of *100nm* was considered for *SEM* images **(a)** and **(b)**. The layers are continuous on the bottom, and become less continuous and develop rugosity on top side.

Figure.3: *X*-ray diffraction patterns of the elaborated absorber designs **(a)** conventional *ITO/a-Si/Glass* structure **(b)** optimized *a-Si/Ti* multilayer absorber with $t_{Absorber}=180nm$ and $t_{ITO}=25nm$.

Figure.4: (a) Absorbance spectra of the prepared *ITO/a-Si* and *a-Si/Ti* multilayer samples with $t_{Absorber}=180nm$ and $t_{ITO}=25nm$. **(b)** Absorption coefficient versus photon energy and **(c)** Tauc plots of the elaborated absorbers based on *ITO/a-Si* and *a-Si/Ti* multilayer structures**.**

Figure.5: (a) Absorbance spectra of 1-sun irradiated absorber based on *a-Si/Ti* multilayer with different illumination periods. **(b)** Variation of the total absorbance efficiency associated with the proposed multilayer structure as a function of the irradiation time.

Figure.6: (a) Device structure with Schottky diode configuration for *I-V* measurements. Measured *I-V* characteristic in logarithmic scale of the fabricated structures based on conventional *ITO/a-Si/Glass* and optimized *a-Si/Ti* multilayer structures under **(b)** dark and **(c)** *1*-sun exposure conditions with $t_{Absorber}=180nm$, $j=5$ and $t_{ITO}=25nm$. The inset figure shows the camera image associated with the elaborated sample based on *a-Si/Ti* multilayered structure.

Tables:

Table.1: Electrical parameters of the elaborated absorbers based on *ITO/a-Si* and *a-Si/Ti* multilayer structures.

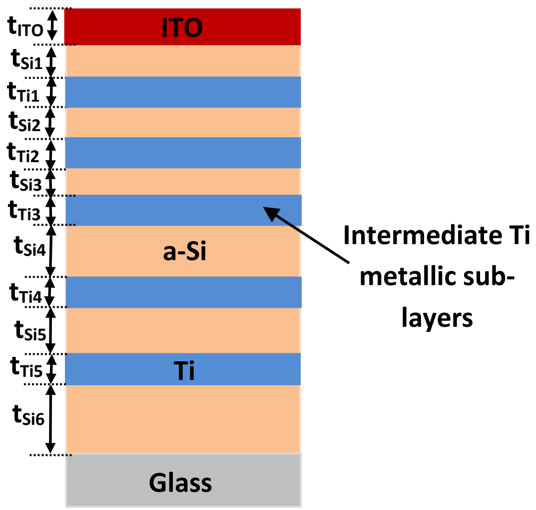
ITO
a-Si
Ti
Glass
Intermediate Ti metallic sub-layers

(a)

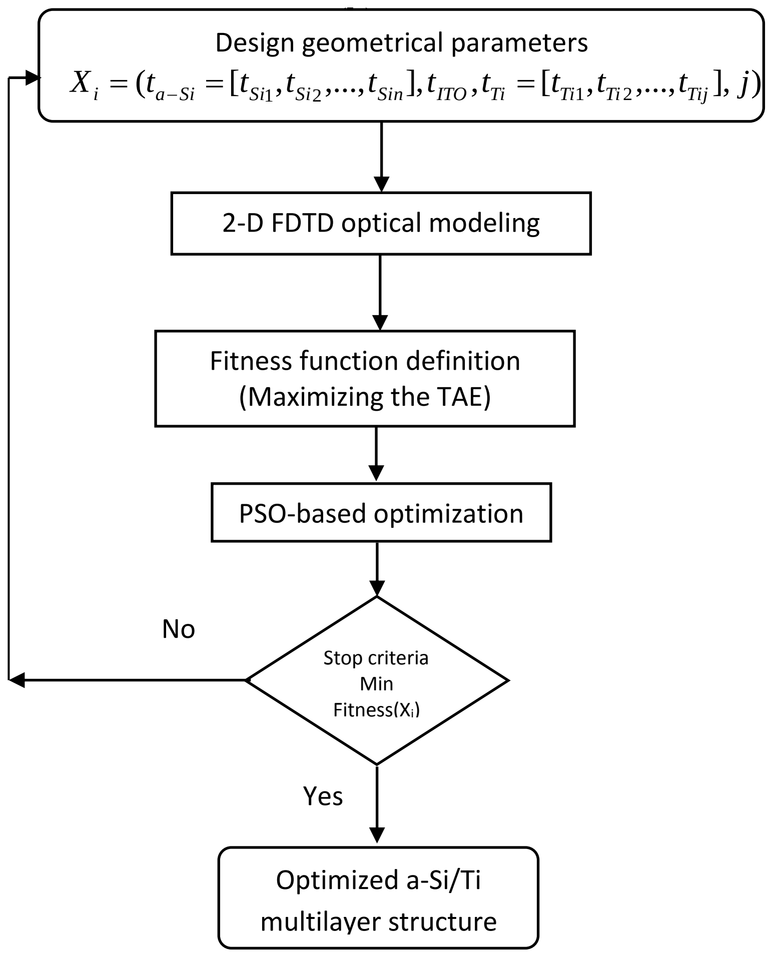
Design geometrical parameters
$X_i = (t_{a-Si} = [t_{Si1}, t_{Si2}, ..., t_{Sin}], t_{ITO}, t_{Ti} = [t_{Ti1}, t_{Ti2}, ..., t_{Tij}], j)$
2-D FDTD optical modeling
Fitness function definition (Maximizing the TAE)
PSO-based optimization
Stop criteria Min Fitness(X_i)
No
Yes
Optimized a-Si/Ti multilayer structure

(b)

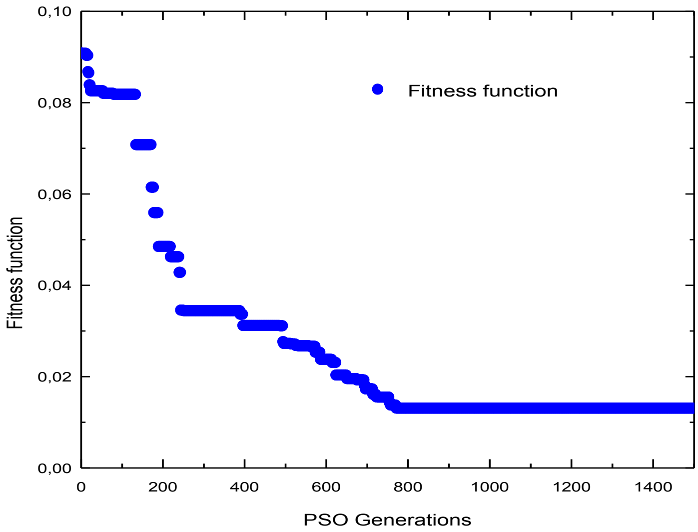
0,10
0,08
0,06
0,04
0,02
0,00
Fitness function
0
200
400
600
800
1000
1200
1400
PSO Generations
Fitness function

(c)

Figure.1

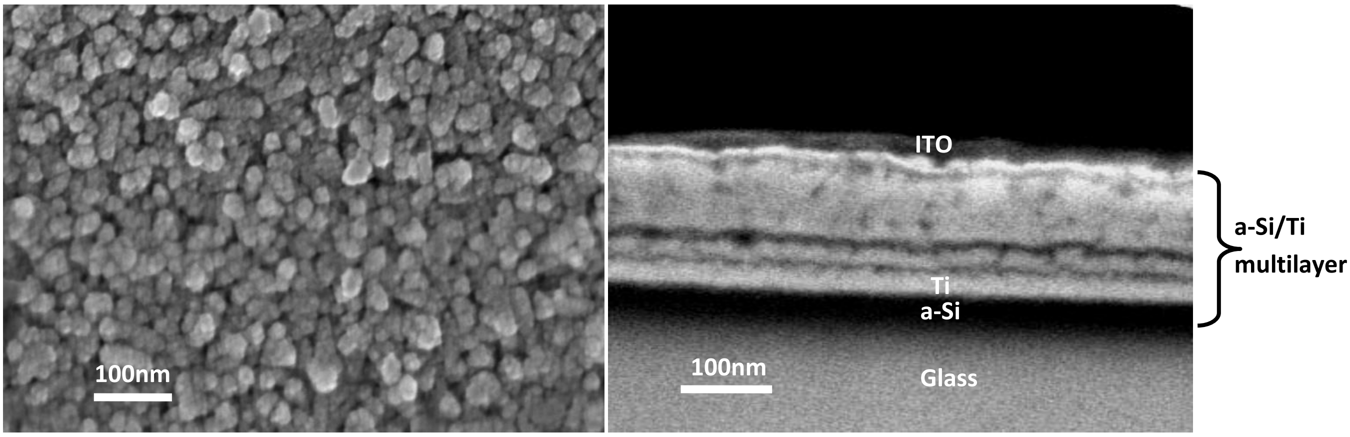

(a) **(b)**

Figure.2

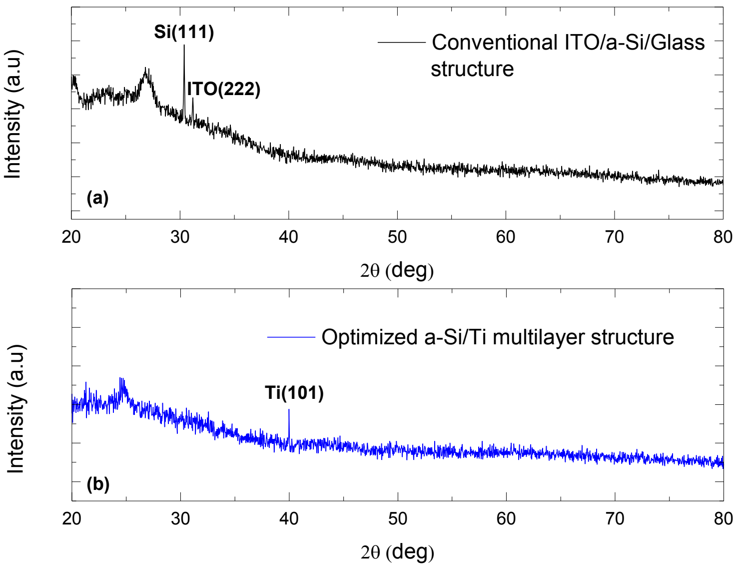
Si(111)
ITO(222)
Conventional ITO/a-Si/Glass structure
Intensity (a.u)
(a)
20
30
40
50
60
70
80
2θ (deg)
Optimized a-Si/Ti multilayer structure
Ti(101)
Intensity (a.u)
(b)
20
30
40
50
60
70
80
2θ (deg)

Figure.3

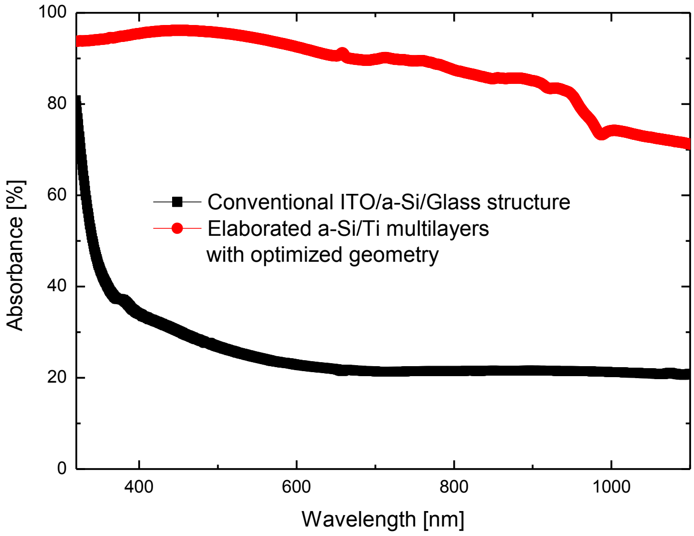
Absorbance [%]
Wavelength [nm]
Conventional ITO/a-Si/Glass structure
Elaborated a-Si/Ti multilayers
with optimized geometry

(a)

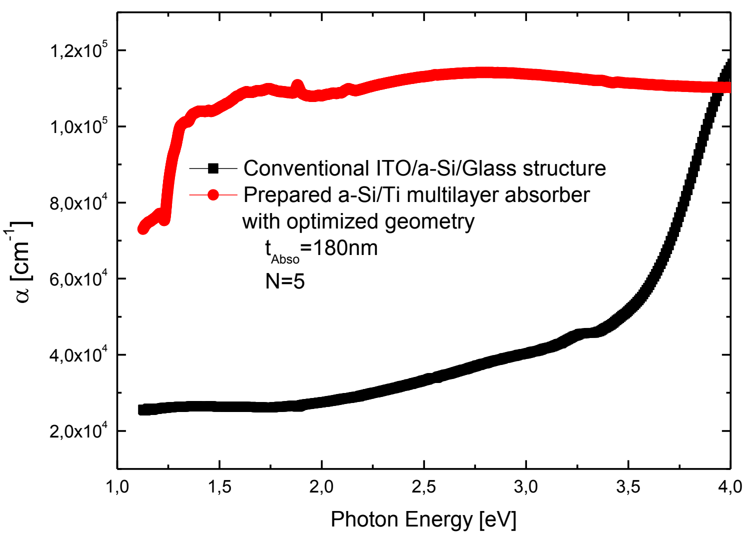
α [cm-1]
Photon Energy [eV]
Conventional ITO/a-Si/Glass structure
Prepared a-Si/Ti multilayer absorber
with optimized geometry
tAbso=180nm
N=5

(b)

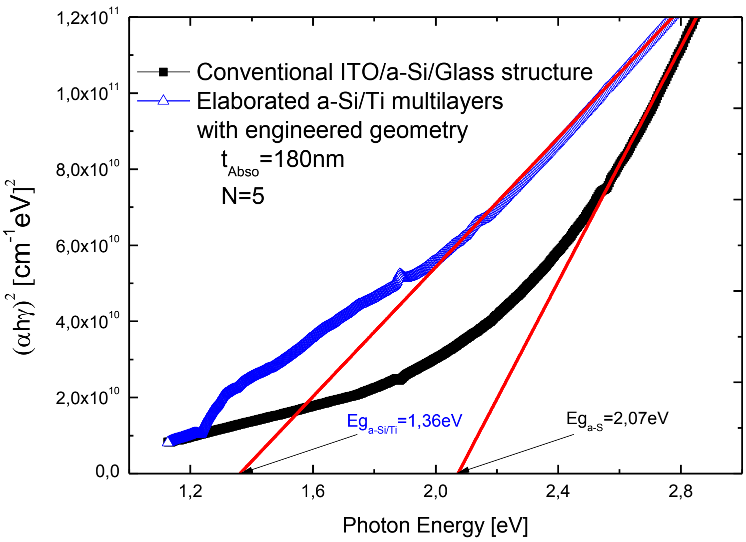

1,2x10^11
1,0x10^11
8,0x10^10
6,0x10^10
4,0x10^10
2,0x10^10
0,0
(αhγ)^2 [cm^-1eV]^2
1,2
1,6
2,0
2,4
2,8
Photon Energy [eV]
Conventional ITO/a-Si/Glass structure
Elaborated a-Si/Ti multilayers
with engineered geometry
t_Abso=180nm
N=5
Eg_a-Si/Ti=1,36eV
Eg_a-S=2,07eV

(c)

Figure.4

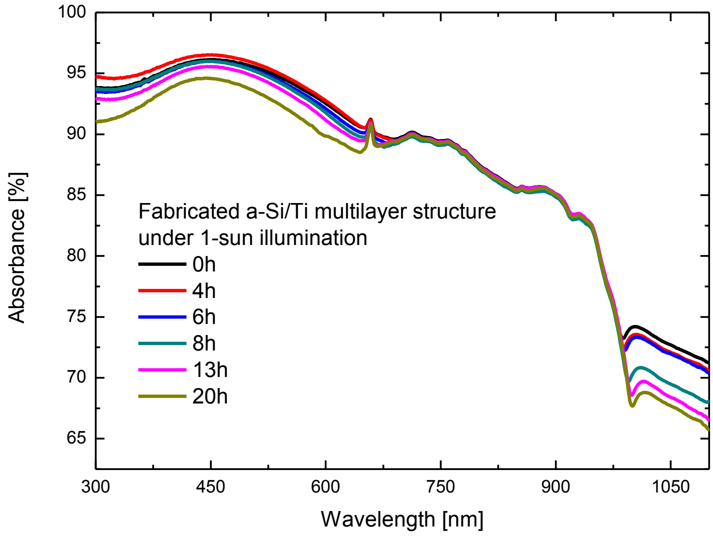
100
95
90
85
80
75
70
65
300
450
600
750
900
1050
Absorbance [%]
Wavelength [nm]
Fabricated a-Si/Ti multilayer structure
under 1-sun illumination
0h
4h
6h
8h
13h
20h

(a)

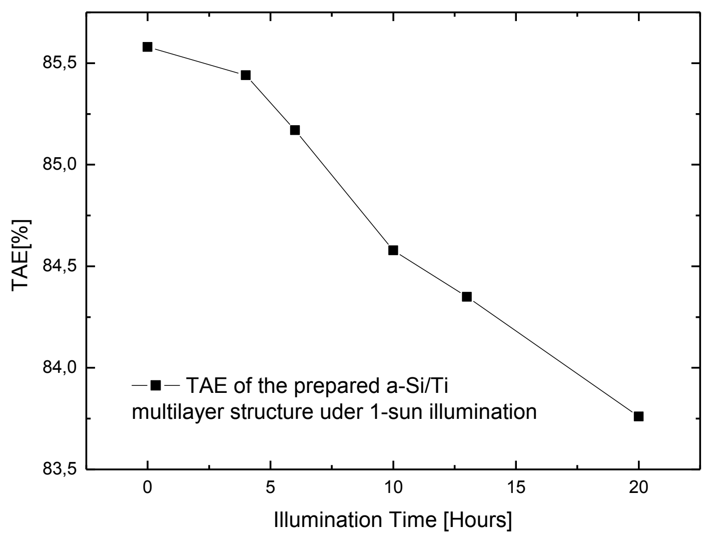
85,5
85,0
84,5
84,0
83,5
0
5
10
15
20
TAE[%]
Illumination Time [Hours]
TAE of the prepared a-Si/Ti
multilayer structure uder 1-sun illumination

(b)

Figure.5

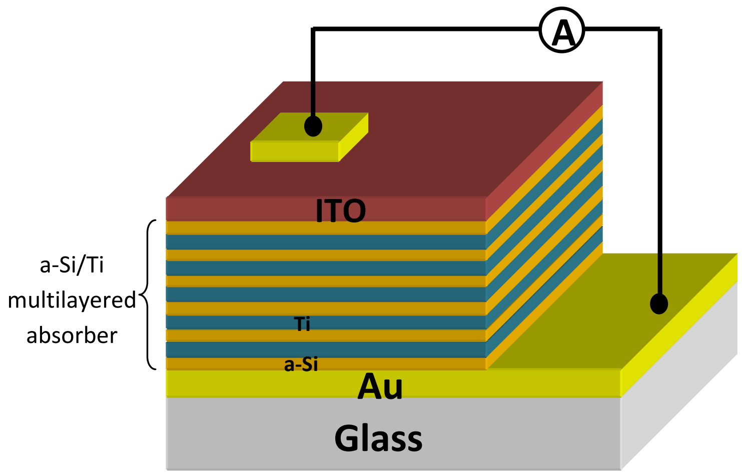
A
ITO
a-Si/Ti
multilayered
absorber
Ti
a-Si
Au
Glass

(a)

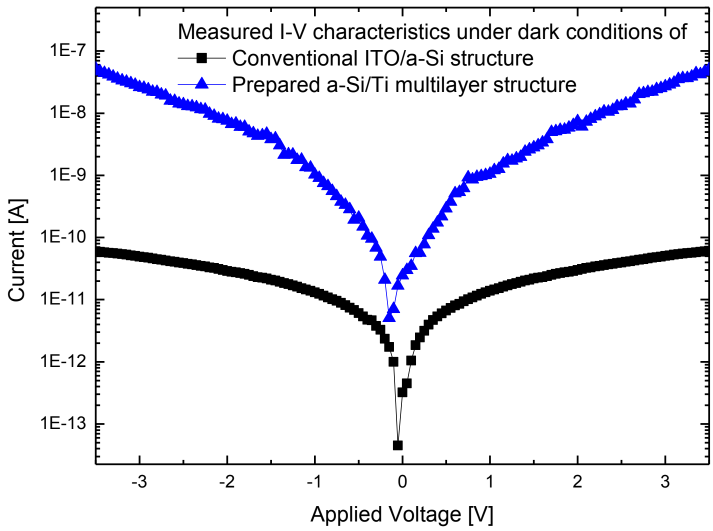
Measured I-V characteristics under dark conditions of
Conventional ITO/a-Si structure
Prepared a-Si/Ti multilayer structure
Current [A]
Applied Voltage [V]
1E-7
1E-8
1E-9
1E-10
1E-11
1E-12
1E-13
-3
-2
-1
0
1
2
3

(b)

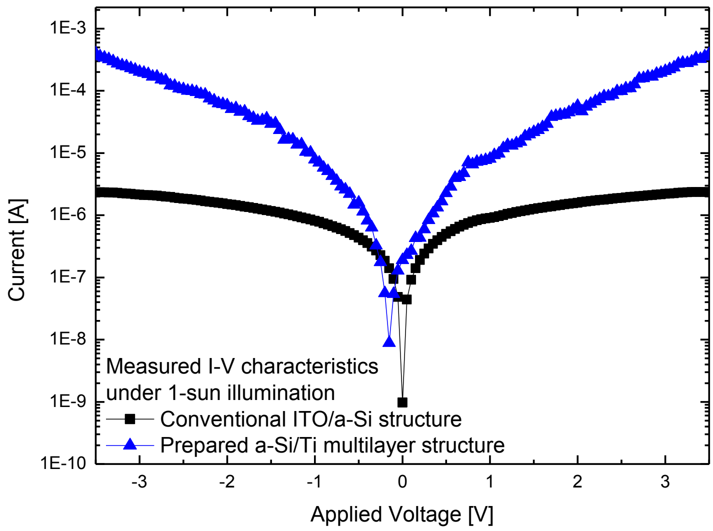

1E-3
1E-4
1E-5
1E-6
1E-7
1E-8
1E-9
1E-10
Current [A]
-3
-2
-1
0
1
2
3
Applied Voltage [V]
Measured I-V characteristics
under 1-sun illumination
Conventional ITO/a-Si structure
Prepared a-Si/Ti multilayer structure

(c)

Figure.6

Table.1

Electrical parameters	**Ideality Factor**	**Schottky barrier height (eV)**	**Series resistance (Ω)**	**Saturation current (nA)**
Conventional *ITO/a-Si* structure	5.85	0.5	1.14×10^{6}	0.97
Prepared *a-Si/Ti* multilayer structure	5.42	0.72	8.63×10^{3}	8.9